2022 IEEE 5th International Conference on Soft Robotics (RoboSoft)
April 4-8, 2022, Edinburgh, UK

Anisotropic Forces for a Worm-Inspired Digging Robot

Dylan Drotman[1], Shivam Chopra[1], Nick Gravish[1], and Michael T. Tolley[1]

Abstract— **Digging through granular media is a challenging problem largely because researchers have limited understanding about how granular intruders interact with granular material. In this work, we designed a bioinspired soft digging robot inspired by polychaete worms (or bristle worms) that used reciprocal elongation and contraction to dig through granular material. Our study investigated the use of asymmetric features for producing anisotropic friction to achieve directed motion. Setae-inspired flexible structures and "terra"foils (i.e. surfaces for robot locomotion in sand) were attached to the robot to produce forward movement and to keep the robot submerged under the granular media, respectively. The robot was actuated by four air-powered longitudinal muscles enabling the robot to extend 24% of its body length when actuated at 138 kPa (20 psi). Our bioinspired robot dug forward under 4 cm of particles and turned on the top surface 24° relative to the longitudinal axis of the robot after 60 seconds. This work represents a step towards worm-inspired subterranean robots that can effectively navigate through granular media.**

I. INTRODUCTION

Digging through granular media (i.e. sand and rubble) is a challenging problem. Researchers have used wheeled robotic systems [1]–[3] and legged robotic systems with compliant feet [4]–[6] to navigate over the surface of granular environments. However, locomotion within granular media is challenging because intruders have to overcome high drag forces [7]. Further, granular media behaves like a solid below the yield stress limit and like a fluid above it [8]. In some cases, electromechanical systems can fail under densely packed grains that resist movement. The forces experienced by an intruder in granular media increases linearly with depth and the performance of robots in granular media changes as the packing fraction changes [4]. Digging robots must be able to produce considerable force to move forward at even modest depths. Furthermore, variance in the environmental conditions (e.g., sand compaction, granule size, and granule material type) has a large impact on the movement of path-generating subterranean mobile systems.

Nature provides examples of designs that can be used to tackle the challenging problem of navigating granular environments. Animals and plants have evolved to dig efficiently in granular environments, providing insights for developing digging robots [9]–[13]. Researchers have developed pneumatically actuated worm robots and snake-inspired robots that can crawl through confined spaces using bioinspired undulatory gaits [14], [15]. Researchers have analyzed the chisel-like shape of the sandfish head to characterize lift and drag forces for subsurface digging [16]. In addition, researchers have designed burrowing robots inspired by plant roots [17], [18].

Worms move their compliant bodies using peristaltic gaits to dig through soil. Body movements enable worms to build large intricate tunnels for surviving in densely packed granular environments [19]–[21]. Polychaete worms generate peristaltic and undulatory gaits through coordinated activation of circular muscles and longitudinal muscles to navigate challenging environments [22]. Polychaete worms use appendages called parapodia to produce thrust for digging and burrowing in sandy environments [23]. These parapodia have stiff structures called setae resembling hairs or bristles to increase traction when the worms are moving in granular media [24].

Worms have been used as inspiration for designing robots that used undulatory robotic locomotion strategies to navigate granular substrates [14], [25]–[28]. In addition, researchers have designed burrowing robots that evert in granular media [18]. These digging robots have either been limited to mobility on the top surface of granular material, or the robots were only able to move in one direction. In recent work, researchers developed a steerable pneumatically actuated everting soft robot that can control subterranean lift and drag forces using local fluidization [12]. This robot requires multiple actuation systems (i.e., a pneumatic system to evert forward and fluidize the sand locally, tendons for controlling the position of the robot, and a motor for retracting the robot). This use of multiple types of actuation leads to multiple potential points of failure when operating in a demanding subterranean environment. In addition, it is difficult to develop self-contained systems when there are multiple actuation methods.

Intruders that move horizontally within granular materials experience both a horizontal drag and a vertical lift force. These resistive forces increase linearly with the increase in depth [29]. A peculiar feature of granular substrates is that granular media generates upward lift forces for many intruder geometries. If the lift force is not counteracted, mobile subterranean systems will veer towards the granular surface rather than digging through the granular media [29]–[31]. This upward lift force makes it challenging to design digging robots that can stay submerged in a plane parallel to the sand surface. Previous work has addressed this problem with an asymmetric nose morphology inspired by the sandfish [16]. In addition to using a similar morphology for the head of our robot, in this work we introduce a new design feature that we call a "terra"foil to solve this problem. The terrafoils are designed to change lift and drag forces on a submerged body to ensure that the robot remains underneath the granular

[1] These authors are with the Department of Mechanical Engineering at the University of California, San Diego (UCSD), 9500 Gilman Dr, La Jolla, CA 92093 USA.

2022 IEEE 5th International Conference on Soft Robotics (RoboSoft) | 978-1-6654-0828-8/22/$31.00 ©2022 IEEE | DOI: 10.1109/ROBOSOFT54090.2022.9762155

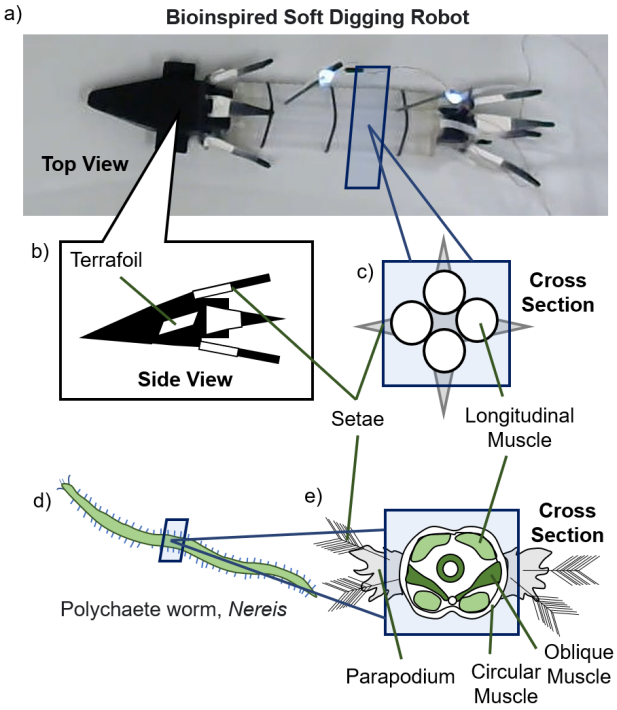

Fig. 1. Bioinspired air-powered soft digging robot. a) The digging robot used longitudinal artificial muscles and anisotropic friction (i.e. setae and terrafoils) to move through granular media. b) The four longitudinal artificial muscles extend when pressurized with air. c) Cross section of the robot showing four longitudinal muscles and two pairs of setae. d) The design and actuation of the robot was inspired by polychaete worms. Polychaete worms generate peristaltic gaits for digging and burrowing in soil by contracting their muscles oriented along the length of their bodies and moving their parapodium and setae to grip the soil. e) Cross section of the polychaete worm showing longitudinal muscles, parapodia and setae.

surface.

In this work, we developed a bioinspired pneumatically actuated robot that digs through granular media (Figure 1a-b). The robot design was inspired by polychaetes (or bristle worms) (Figure 1c-e). In Section I, we discuss the design and fabrication of the worm-inspired robot. We describe how the design of the setae and "terra"foils affect the lift force and drag force on the robot while digging under granular media. In Section III, we demonstrate the digging and steering capabilities of the robot. In Section IV and V, we discuss future work and conclude our study.

II. DESIGN AND FABRICATION

A. Robot Design

Our worm-inspired robot used four air-powered longitudinal muscles and directional friction from terrafoils and setae to dig through sand. The bioinspired robot was designed to push forward (i.e. the front setae fold in, Phase 1 and 2) and pull forward (i.e. the back setae fold in, Phase 3 and 4) (Figure 2a). In Phase 1, the four longitudinal muscles are pressurized and in Phase 3, the four longitudinal muscles are depressurized. We used an inflation and deflation timing sequence to control the robot gait sequence. The inflation and deflation sequence was repeated to produce forward movement.

The forward movement was made possible due to the directional friction attached to the surface of the robot (i.e. terrafoils and setae). Inspired by setae in bristle worms, we designed anisotropic setae structures to bend towards the robot when the robot pushes forward and then become stiff to resist backward movement. Four setae were equally distributed around the front and back of the robot.

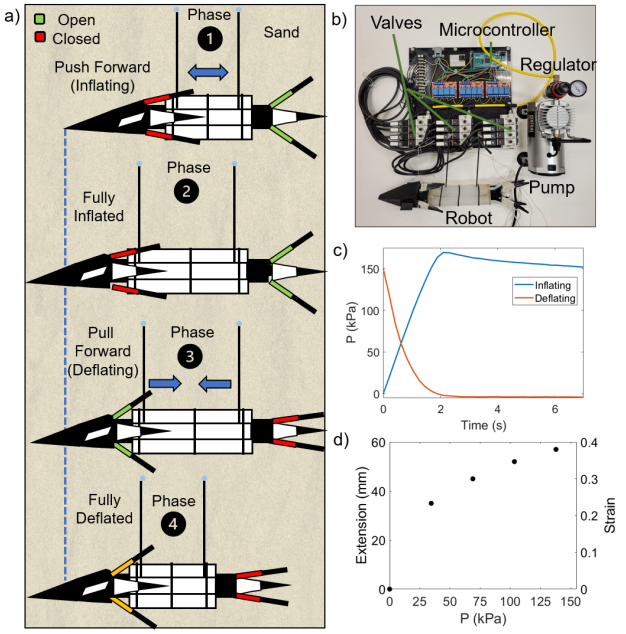

Fig. 2. Experimental setup for controlling the bioinspired digging robot. a) Four phase gait sequence to control forward movement. b) Pneumatic control system used to control the pressure in the air-powered artificial muscles. c) Inflation and deflation dynamics when one of the artificial muscles was actuated from the pressure-regulated pump. The pressure saturated after 2 seconds for the deflation and inflation phase. d) Relationship between pressure and the extension of each longitudinal muscle.

In this work, we introduce a new submerged surface which we call a "terra"foil. The terrafoils were designed to control the lift and drag forces on a body that is submerged in sand. Digging through sand produces different effects on the submerged body. Firstly, granular media introduces a significant amount of drag on submerged bodies. In addition, the resistive forces in sand increase linearly with the depth and thus intruders experience an upward lift force. This can cause symmetric subterranean mobile systems to gradually move up towards the surface of the sand [16].

We attached terrafoils on both sides of the head of the robot to ensure the robot would not ascend from the sand by producing a downward force when the robot moved forward. Since terrafoils add additional drag to the front of the robot, we offset this drag by reducing the projected cross-sectional area of the front setae. The cross-sectional projected area of the front setae ($A_{FS} = 1244$ mm^2) plus the area of the terrafoils at a 15° angle ($A_{15T} = 410$ mm^2) summed up to the total cross-sectional projected area of the setae at the back of the robot ($A_{BS} = 1654$ mm^2).

The head of the robot was inspired by the wedge-shaped head of the sandfish. Previous work showed that the angle of the head of a sandfish-inspired robot changed lift and drag forces which enabled the robot to remain submerged [16]. In this work, we used a head design that introduced the most downward force ($h/H = 1/8$, $L = 2.14H$ where H is the height of the wedge, h is the height from the bottom of the head to the tip, and L is the length of the wedge) to keep the robot submerged.

Three O-rings held the four artificial muscles together. 3D printed mounts connected the artificial muscles to the head of the robot and the setae. The terrafoils were attached to the side of the head of the robot. Each of the setae were lasercut out of acrylic and bonded to taffeta sheets. The bonded setae were wrapped with a latex balloon to provide an elastic restoring force to reset the setae for each gait cycle.

To activate the artificial muscles, the robot was connected by silicone tubes to a pneumatic control board (Figure 2b). The pneumatic timing was controlled using a microcontroller, electromechanical valves, and a pressure-regulated pump. When the chambers were actuated at 138 kPa (20 psi), the robot body extended 24% of the body length. The body length was measured from the base of the chambers to the end of the chambers. Pressure saturated after 2 seconds during the deflation and inflation phases (Figure 2c). The pressure in the chamber was used to control the extension of each longitudinal muscle (Figure 2d).

In Section IIB and IIC, we describe experiments we conducted to measure lift and drag forces on the setae and terrafoils. We submerged the robot elements (i.e each terrafoil design or each setae design) in dry granular media to a 4 cm depth. The dry sand was fluidized (i.e. the packing fraction was reset) before each experiment was performed.

In addition, we describe experiments in Section IIIA where we tested each setae and terrafoil design on the robot by measuring the initial and final position of the robot after digging through dry granular media. Each of the robot digging experiments were performed at 4 cm depth. The robot was actuated in sequence during the digging experiments; all four artificial muscles on the robot were inflated for 2 seconds and then deflated for 4 seconds. The pressure was regulated to 138 kPa (20 psi). At the start of each robot experiment, the robot was pushed back until the setae were reset (i.e. fully open). The position measurements were recorded at 3 Hz.

B. Terrafoil Design Study

The drag and lift along the body of a submerged object depends on the objects shape, orientation, surface roughness, and depth. The equation for drag and lift on a submerged objects is [32]:

$$F_{z,x} = \int_S \sigma_{z,x}(\alpha, \gamma_s)|z|_s dA_s \tag{1}$$

where S is the leading surface area of the object; dA_s, $|z|_s$, α, and γ_s are the area, depth below the surface, angle of attack, and the angle of intrusion of infinitesimal elements; and $\sigma_{z,x}(\beta_s, \gamma_s)$ are the element stresses per unit depth. Equation 1 shows that the cross-sectional area of a submerged object has a significant impact on the overall drag experienced by the robot. The cross-section of the submerged object has a larger impact compared to skin drag (i.e. the drag along the length of the submerged body). The drag force and lift force on the body can be tuned by changing the angle attack of the submerged object. This fundamental principle is what was used to tune the design for the subterranean digging robot.

We designed terrafoils to counteract forces that cause subterranean mobile systems to move towards the surface. The terrafoils were designed to push the robot down into the sand, however, we hypothesized that too much downward force could cause the robot to move slowly or anchor. To test this hypothesis, we dragged two different terrafoil designs (α = 5° and α = 15°) forward and backward through granular media and measured the drag and lift force for each trial (Figure 3b-c). Each of the terrafoils were the same size (30 mm × 20 mm × 2 mm). The terrafoils were attached to a linear stage that dragged the terrafoils through sand at a 4 cm depth (Figure 3a).

When the terrafoils were dragged backwards using the linear stage, the 15° terrafoil had a larger drag force when compared to the 5° terrafoil which matches the predictions from Resistive force theory (RFT) [33]. Lift force results show that the 15° terrafoil produced more downward force than the 5° terrafoil when dragged forward. These results highlight the benefit of adding terrafoils to the robot; the terrafoils help to keep the robot submerged while also providing asymmetric friction for forward locomotion. The angle of the terrafoil has to be carefully tuned to assess the trade-off between less drag when the robot pushes forward and high drag when the robot pulls backwards.

C. Artificial Setae Design Study

Worms have adapted to life underground by developing features for burrowing in densely packed soil. Worms create motion and build tunnels by activating parapodia covered with bristle-like setae that are designed to grip the soil [24], [34]. The setae on our worm-inspired robot were designed to behave like an anchor when the setae opened up (i.e. opened away from the robot body). The acrylic elements pushed against each other preventing the setae from bending. Conversely, the setae were designed to be flexible when the setae folded towards the body of the robot (Figure 4a). The anisotropic friction provided from the setae enabled the robot to move forward during each gait cycle.

Our hypothesis was that the angle θ (i.e. the angle of the setae relative to the longitudinal axis of the robot) changes the amounts of anisotropic friction which affects how well the robot can dig through sand (Figure 4a). To answer this question, we varied the angle θ and dragged each setae forwards and backwards through sand to observe the differences in lift and drag forces (Figure 4c-d).

The results showed that the lower angle setae (30°) provided less drag force forward and backward when compared to the higher angle setae (45°) (Figure 4c). For the front

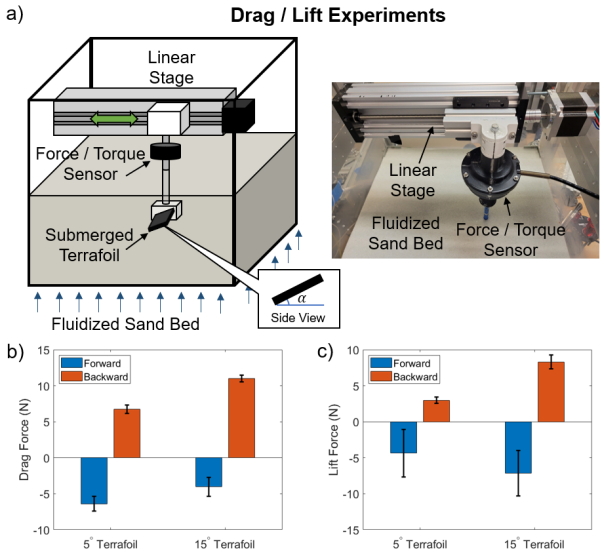

Fig. 3. Terrafoil test setup for measuring lift and drag forces. a) Experimental setup for measuring lift and drag forces on a submerged terrafoil. b) Drag force measurements when the 5° and 15° terrafoil were dragged forwards and backwards. b) Drag force measurements when 5° and 15° terrafoil was horizontally moved in forward and backward directions. c) Lift force measurements for the same experiment.

setae, the optimal design needs a drag force that is lower than the force generated from the robot when the robot pushes forward (Phase 1) and a drag force that is higher than the force generated from the robot when the robot pulls forward (Phase 3). The opposite is true for the back setae since the back setae anchors in Phase 1 and folds in during Phase 3.

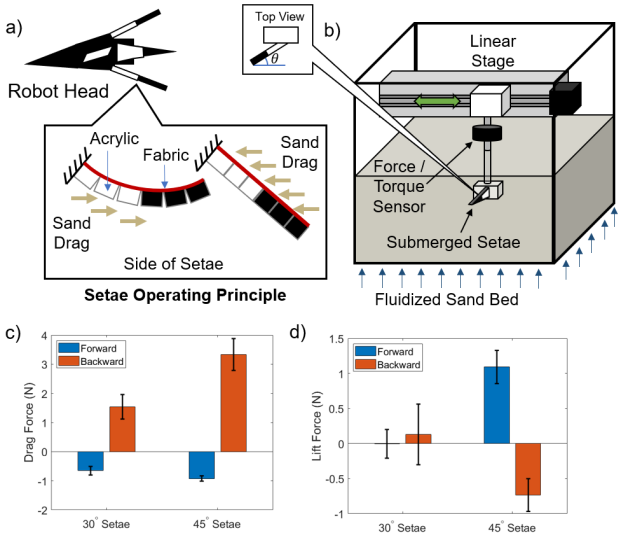

Fig. 4. Setae test setup for measuring lift and drag forces. a) Schematic of the bioinspired robot with varying setae angle θ. The inset shows the design of the anisotropic setae bending backwards to reduce drag when the robot was moving forward and becoming straight to increase asymmetric drag for generating net propulsion b) Schematic of the experimental setup. c) Drag forces on the 30° setae and the 45° setae when the setae was dragged forward and backward. d) Lift forces from the same experiment

III. DIGGING EXPERIMENTS

A. Forward Digging

To understand how the setae and terrafoils impact locomotion, we attached different pairs of setae and terrafoils to the robot and actuated the robot gait sequence for 150 s. We observed the changed in horizontal and vertical position of the robot as the robot dug forward (Figure 5a-d). We compared these results for the 5° terrafoil and the 15° terrafoil (both tests with 45° setae) to analyze how terrafoils with different angles affected locomotion (Figure 5a-b) and we compared the 30° setae and 45° setae (both tests with 5° terrafoil) how different setae affected locomotion (Figure 5c-d).

The robot with the 15° terrafoil was slower than the robot with the 5° terrafoil. We believe this is because the 15° terrafoil introduced more drag. (Figure 5a). The robot with the 5° terrafoil and the 15° terrafoil emerged from the sand about the same amount after 150 s (Figure 5b).

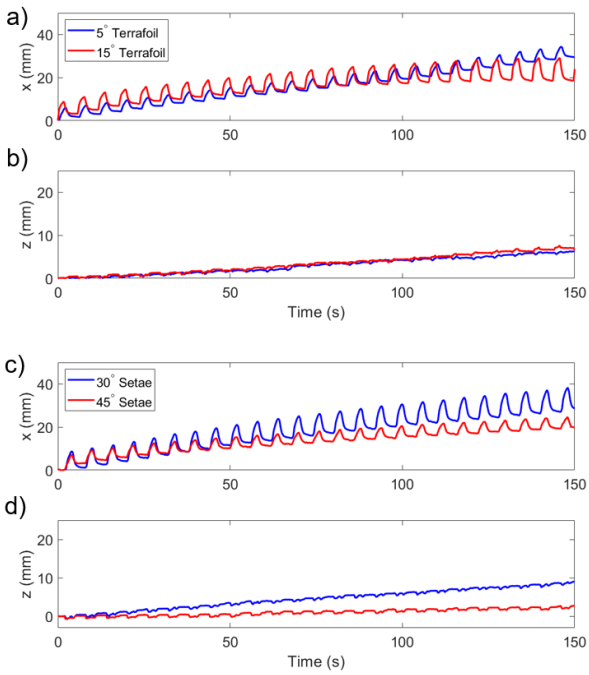

Fig. 5. Forward digging with different robot configurations. The x-direction represents forward displacement, and z-direction represents depth where the 0 location is the initial position of the robot at 4 cm depth. We tracked the position of the robot by tracking led lights attached to the robot that were raised above the sand surface. a-b) The robot with the 5° terrafoil dug further than the robot with the 15° terrafoil in 150 s. The robots with the 5° and 15° terrafoils emerged from the sand about the same amount. Both experiments were tested using 45° setae. c-d) The robot with the 30° terrafoil dug further than the robot with the 30° setae in 150 s. In addition, we observed that the robot with the 30° setae moved vertically out of the sand more than the robot with the 45° setae. Both experiments were tested using 5° terrafoils.

The robot with the 30° setae made more forward progress after 150s than the robot with the 45° setae (Figure 5c). We believe this is because the 30° setae folded closer to the body of the robot during the gait sequence. It was unexpected that

the robot with the 30° setae emerged from the sand more than the 45° setae. Before running the experiments, we assumed the change in z height of the robot with the 30° setae and the robot with the 45° setae would be similar. We believe the setae twisted about the longitudinal axis of the setae due to slight differences in the way the setae were mounted.

B. Robot Steering

We ran experiments to test different steering approaches. To make the robot turn, one of the four longitudinal artificial muscles could be inflated (i.e. the robot would bend away from the inflated chamber) or three of the artificial muscles could be inflated simultaneously (i.e. the top, bottom and a side chamber could be actuated to bend away from the side chamber) (Figure 6a).

We first measured the bending angle of the robot body in sand at a 4 cm depth and out of sand when one chamber was activated at different pressures (Figure 6b). The robot body bent 60° out of sand and 51° in sand at a 4 cm depth when inflated to 200 kPa.

To compare the three chamber and single chamber steering methods, we measured the magnitude of the force in x and y direction (i.e. forces in the plane of bending) and moment during 3 inflation-deflation cycles and reported the average forces for each actuation cycle (Figure 6c and d). The results showed that it is best to inflate three chambers rather than one chamber at a time to make the robot turn under sand. The additional forces from the three extending chambers (i.e. the top and bottom chambers) increase the force exerted from the robot. The magnitude of the force was 44% larger when three chambers were inflated when compared to one chamber (Figure 6c).

We demonstrated the steering capability of the robot on a the granular surface (Figure 6e-f). To make the robot turn, we activated three chambers in sequence (i.e. three chambers were inflated for 2 seconds and deflated for 4 seconds). To make the robot turn right, we activated the left chamber, top chamber, and bottom chamber. After 60 seconds, the robot turned right 24° relative to the longitudinal axis of the robot. We hypothesize that the robot would turn left a similar amount if the right chamber was activated instead of the left chamber. Although the robot is unable to turn in place, the robot is able to gradually change direction.

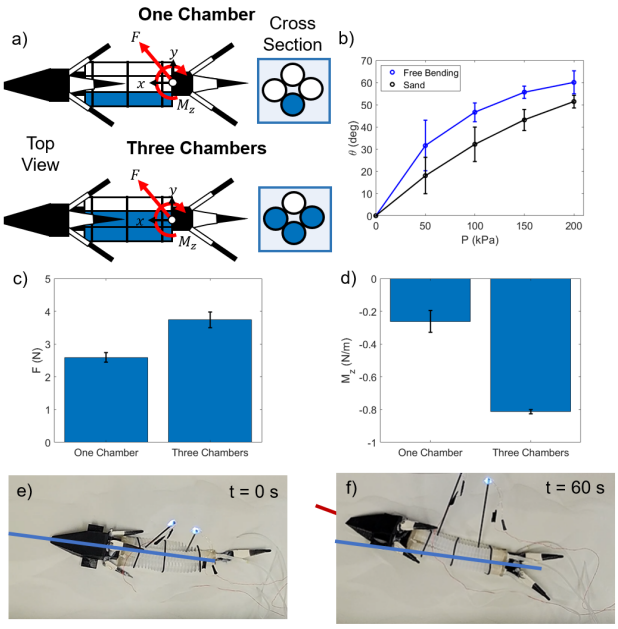

Fig. 6. Robot steering in sand. a) Either one or three chambers on the robot could be inflated at a time to control the direction the robot turns. b) When one chamber was inflated to 200 kPa, the actuator bent 60° out of sand and 51° in sand at a 4 cm depth. c-d) We measured the force magnitude and moment when we inflated one and three chambers and found that three chambers provided more force for digging through sand. e-f) The robot turned right 24° relative to the longitudinal axis of the robot on the sand surface when three chambers were actuated in a periodic sequence for 60s.

IV. FUTURE WORK

There are other appendage designs that may improve some of the qualities of the proposed design. For example, the terrafoil produced a downward force during the forward stroke to prevent the robot from surfacing but it also introduced lift during the backstroke drag. Another design could include mirrored terrafoils (i.e. a terrafoil to keep the robot from emerging during the forward and back stroke) to prevent the robot from surfacing during the backstroke. In addition, the setae are prone to breaking over repeated cycles. There may be a terrafoil design (i.e. a stationary appendage) that could replace the setae (i.e an appendage that bends).

The packing fraction of the sand determines which direction the robot will move since digging robots move along the path of least resistance. When the back of the robot anchored in the sand, the head of the robot emerged to the surface because the sand on the surface was not as compact as the sand beneath the robot. When the front of the robot anchored, the back of the robot moved towards the top surface of the sand.

Under ideal circumstances, the setae would provide minimal lift. However, because the back taffeta layer on each of the setae was flexible, we believe the setae twisted out-of-plane around the base connection to the robot resulting in a lift force (Figure 4d). This mode can be prevented in future designs by adding a stiffer backing or longitudinal reinforcements along the length of the setae.

There are other experiments we could have performed to demonstrate the capabilities of this robot. We could control vertical mobility of the robot by activating the top and bottom artificial muscle separately. In addition, we did not vary the depth for the experiments in this work but we suspect the robot would be able to move through granular media at other depths. Polycheate worms have multiple segments to move through a variety of environments. Our robot only used one segment to generate a peristaltic gait, however, future designs could include more segments to produce a traveling wave gait for coordinated lateral movements.

V. CONCLUSIONS

The air-powered bioinspired digging robot proposed in this work stayed beneath the sand surface by utilizing the downward force produced by terrafoils and directional friction from setae-inspired appendages. This work builds an understanding about how these appendages affect the mobility of subterranean robotic systems.

ACKNOWLEDGMENT

This material is based upon work supported by the Office of Naval Research under grant number N00014-20-1-2373. Any opinions, findings, and conclusions or recommendations expressed in this material are those of the author(s) and do not necessarily reflect the views of the ONR.

REFERENCES

[1] J. Wong, "On the study of wheel-soil interaction," *Journal of Terramechanics*, vol. 21, no. 2, pp. 117–131, 1984.

[2] P. Lamon and R. Siegwart, "Wheel torque control in rough terrain-modeling and simulation," in *Proceedings of the 2005 IEEE international conference on robotics and automation*, pp. 867–872, IEEE, 2005.

[3] L. Ding, Z. Deng, H. Gao, K. Nagatani, and K. Yoshida, "Planetary rovers' wheel–soil interaction mechanics: new challenges and applications for wheeled mobile robots," *Intelligent Service Robotics*, vol. 4, no. 1, pp. 17–38, 2011.

[4] C. Li, P. B. Umbanhowar, H. Komsuoglu, D. E. Koditschek, and D. I. Goldman, "Sensitive dependence of the motion of a legged robot on granular media," *Proceedings of the National Academy of Sciences*, vol. 106, no. 9, pp. 3029–3034, 2009.

[5] D. J. Lynch, K. M. Lynch, and P. B. Umbanhowar, "The Soft-Landing Problem: Minimizing Energy Loss by a Legged Robot Impacting Yielding Terrain," *IEEE Robotics and Automation Letters*, vol. 5, pp. 3658–3665, feb 2020.

[6] S. Chopra, M. T. Tolley, and N. Gravish, "Granular Jamming Feet Enable Improved Foot-Ground Interactions for Robot Mobility on Deformable Ground," *IEEE Robotics and Automation Letters*, vol. 5, pp. 3975–3981, jul 2020.

[7] A. Martinez, J. DeJong, I. Akin, A. Aleali, C. Arson, J. Atkinson, P. Bandini, T. Baser, R. Borela, R. Boulanger, M. Burrall, Y. Chen, C. Collins, D. Cortes, S. Dai, T. DeJong, E. Del Dottore, K. Dorgan, R. Fragaszy, J. D. Frost, R. Full, M. Ghayoomi, D. I. Goldman, N. Gravish, I. L. Guzman, J. Hambleton, E. Hawkes, M. Helms, D. Hu, L. Huang, S. Huang, C. Hunt, D. Irschick, H. T. Lin, B. Lingwall, A. Marr, B. Mazzolai, B. McInroe, T. Murthy, K. O'Hara, M. Porter, S. Sadek, M. Sanchez, C. Santamarina, L. Shao, J. Sharp, H. Stuart, H. H. Stutz, A. Summers, J. Tao, M. Tolley, L. Treers, K. Turnbull, R. Valdes, L. van Paassen, G. Viggiani, D. Wilson, W. Wu, X. Yu, and J. Zheng, "Bio-inspired geotechnical engineering: principles, current work, opportunities and challenges," *Géotechnique*, vol. 0, no. 0, pp. 1–19, 0.

[8] R. M. Nedderman *et al.*, *Statics and kinematics of granular materials*, vol. 352. Cambridge University Press Cambridge, 1992.

[9] R. D. Maladen, Y. Ding, C. Li, and D. I. Goldman, "Undulatory swimming in sand: subsurface locomotion of the sandfish lizard.," *Science (New York, N.Y.)*, vol. 325, pp. 314–8, jul 2009.

[10] A. G. Winter, V, R. L. H. Deits, D. S. Dorsch, A. H. Slocum, and A. E. Hosoi, "Razor clam to RoboClam: burrowing drag reduction mechanisms and their robotic adaptation," *Bioinspiration Biomimetics*, vol. 9, p. 036009, apr 2014.

[11] A. A. Calderon, J. C. Ugalde, J. C. Zagal, and N. O. Perez-Arancibia, "Design, fabrication and control of a multi-material-multi-actuator soft robot inspired by burrowing worms," in *2016 IEEE International Conference on Robotics and Biomimetics (ROBIO)*, pp. 31–38, IEEE, dec 2016.

[12] N. D. Naclerio, A. Karsai, M. Murray-Cooper, Y. Ozkan-Aydin, E. Aydin, D. I. Goldman, and E. W. Hawkes, "Controlling subterranean forces enables a fast, steerable, burrowing soft robot," *Sci. Robot*, vol. 6, p. 2922, 2021.

[13] H. Wei, Y. Zhang, T. Zhang, Y. Guan, K. Xu, X. Ding, and Y. Pang, "Review on bioinspired planetary regolith-burrowing robots," *Space Science Reviews*, vol. 217, no. 8, pp. 1–39, 2021.

[14] Y. Ozkan-Aydin, B. Liu, A. C. Ferrero, M. Seidel, F. L. Hammond, and D. I. Goldman, "Lateral undulation aids biological and robotic earthworm anchoring and locomotion," *bioRxiv*, 2021.

[15] X. Qi, H. Shi, T. Pinto, and X. Tan, "A novel pneumatic soft snake robot using traveling-wave locomotion in constrained environments," *IEEE Robotics and Automation Letters*, vol. 5, no. 2, pp. 1610–1617, 2020.

[16] R. D. Maladen, P. B. Umbanhowar, Y. Ding, A. Masse, and D. I. Goldman, "Granular lift forces predict vertical motion of a sand-swimming robot," in *2011 IEEE International Conference on Robotics and Automation*, pp. 1398–1403, 2011.

[17] A. Sadeghi, A. Mondini, and B. Mazzolai, "Toward self-growing soft robots inspired by plant roots and based on additive manufacturing technologies," *Soft Robotics*, vol. 4, no. 3, pp. 211–223, 2017. PMID: 29062628.

[18] A. Sadeghi, A. Tonazzini, L. Popova, and B. Mazzolai, "Robotic mechanism for soil penetration inspired by plant root," in *2013 IEEE International Conference on Robotics and Automation*, pp. 3457–3462, 2013.

[19] K. M. Dorgan, P. A. Jumars, B. Johnson, B. P. Boudreau, and E. Landis, "Burrow extension by crack propagation," *Nature*, vol. 433, p. 475, feb 2005.

[20] K. M. Dorgan, "The biomechanics of burrowing and boring," *J. Exp. Biol.*, vol. 218, pp. 176–183, jan 2015.

[21] K. M. Dorgan, C. J. Law, and G. W. Rouse, "Meandering worms: Mechanics of undulatory burrowing in muds," *Proceedings of the Royal Society B: Biological Sciences*, vol. 280, no. 1757, 2013.

[22] J. Gray, "STUDIES IN ANIMAL LOCOMOTION VIII. THE KINETICS OF LOCOMOTION OF NEREIS DIVERSICOLOR," tech. rep.

[23] T. Hesselberg and J. F. Vincent, "The function of parapodial setae in a nereidid polychaete moving on two different substrata," *Journal of Experimental Marine Biology and Ecology*, vol. 335, no. 2, pp. 235–244, 2006.

[24] T. Hesselberg and J. F. Vincent, "The function of parapodial setae in a nereidid polychaete moving on two different substrata," *Journal of Experimental Marine Biology and Ecology*, vol. 335, pp. 235–244, aug 2006.

[25] D. P. Tsakiris, M. Sfakiotakis, A. Menciassi, G. La Spina, and P. Dario, "Polychaete-like undulatory robotic locomotion," in *Proceedings of the 2005 IEEE International Conference on Robotics and Automation*, pp. 3018–3023, IEEE, 2005.

[26] H. Marvi, C. Gong, N. Gravish, H. Astley, M. Travers, R. L. Hatton, J. R. Mendelson, H. Choset, D. L. Hu, and D. I. Goldman, "Sidewinding with minimal slip: Snake and robot ascent of sandy slopes," *Science*, vol. 346, no. 6206, pp. 224–229, 2014.

[27] W. Baumgartner, F. Fidler, A. Weth, M. Habbecke, P. Jakob, C. Butenweg, and W. Böhme, "Investigating the locomotion of the sandfish in desert sand using nmr-imaging," *PLOS ONE*, vol. 3, pp. 1–10, 10 2008.

[28] B. Liu, Y. Ozkan-Aydin, D. I. Goldman, and F. L. Hammond, "Kirigami skin improves soft earthworm robot anchoring and locomotion under cohesive soil," in *2019 2nd IEEE International Conference on Soft Robotics (RoboSoft)*, pp. 828–833, 2019.

[29] F. Guillard, Y. Forterre, and O. Pouliquen, "Lift forces in granular media," *Physics of Fluids*, vol. 26, no. 4, p. 043301, 2014.

[30] R. D. Maladen, Y. Ding, P. B. Umbanhowar, A. Kamor, and D. I. Goldman, "Mechanical models of sandfish locomotion reveal principles of high performance subsurface sand-swimming," *Journal of The Royal Society Interface*, vol. 8, no. 62, pp. 1332–1345, 2011.

[31] N. D. Naclerio, A. Karsai, M. Murray-Cooper, Y. Ozkan-Aydin, E. Aydin, D. I. Goldman, and E. W. Hawkes, "Controlling subterranean forces enables a fast, steerable, burrowing soft robot," *Science Robotics*, vol. 6, no. 55, 2021.

[32] C. Li, T. Zhang, and D. I. Goldman, "A terradynamics of legged locomotion on granular media," *Science*, vol. 339, no. 6126, pp. 1408–1412, 2013.

[33] C. Li, T. Zhang, and D. I. Goldman, "A terradynamics of legged locomotion on granular media," *Science*, vol. 339, pp. 1408–1412, mar 2013.

[34] T. Hesselberg and J. F. V. Vincent, "A comparative study of the functional morphology of parapodia and setae in nereids (Polychaeta: Nereididae)," Tech. Rep. 1, 2006.